CellPress

Cancer Cell
Article

PKD1 Phosphorylation-Dependent Degradation of SNAIL by SCF-FBXO11 Regulates Epithelial-Mesenchymal Transition and Metastasis

Hanqiu Zheng,[1] Minhong Shen,[1,2] Yin-Lian Zha,[3] Wenyang Li,[1] Yong Wei,[1] Mario Andres Blanco,[4] Guangwen Ren,[1] Tianhua Zhou,[2] Peter Storz,[5] Hui-Yun Wang,[3] and Yibin Kang[1,6,*]

[1]Department of Molecular Biology, Princeton University, Princeton, NJ 08544, USA
[2]Department of Cell Biology and Program of Molecular Cell Biology, Zhejiang University School of Medicine, Hangzhou 310058, China
[3]State Key Laboratory of Oncology in South China, Sun Yat-Sen University Cancer Center, Guangzhou 510060, China
[4]Department of Cell Biology, Harvard Medical School and Division of Newborn Medicine, Boston Children's Hospital, Boston, MA 02115, USA
[5]Department of Cancer Biology, Mayo Clinic, Griffin Building, Room 306, 4500 San Pablo Road, Jacksonville, FL 32224, USA
[6]Genomic Instability and Tumor Progression Program, Rutgers Cancer Institute of New Jersey, New Brunswick, NJ 08903, USA
*Correspondence: ykang@princeton.edu
http://dx.doi.org/10.1016/j.ccr.2014.07.022

SUMMARY

Metastatic dissemination is often initiated by the reactivation of an embryonic development program referred to as epithelial-mesenchymal transition (EMT). The transcription factor SNAIL promotes EMT and elicits associated pathological characteristics such as invasion, metastasis, and stemness. To better understand the posttranslational regulation of SNAIL, we performed a luciferase-based, genome-wide E3 ligase siRNA library screen and identified SCF-FBXO11 as an important E3 that targets SNAIL for ubiquitylation and degradation. Furthermore, we discovered that SNAIL degradation by FBXO11 is dependent on Ser-11 phosphorylation of SNAIL by protein kinase D1 (PKD1). FBXO11 blocks SNAIL-induced EMT, tumor initiation, and metastasis in multiple breast cancer models. These findings establish the PKD1-FBXO11-SNAIL axis as a mechanism of posttranslational regulation of EMT and cancer metastasis.

INTRODUCTION

The majority of cancer-related deaths can be attributed to the spread of cancer cells to distant vital organs (Wan et al., 2013). Epithelial-mesenchymal transition (EMT), a crucial process in embryonic development that allows epithelial cells to lose apical-basal polarity and cell-cell contacts while gaining mesenchymal phenotypes, is believed to be utilized by cancer cells to gain mobility and invasiveness during metastasis (Brabletz, 2012; De Craene and Berx, 2013; Nieto, 2011). A hallmark of EMT is the functional loss of E-cadherin, and additional cellular changes, such as reduced expression of the epithelial markers cytokeratin and ZO-1 and the upregulation of the mesenchymal markers N-cadherin, Vimentin, and Fibronectin, are also observed frequently.

SNAIL protein was among the first transcription factors discovered to repress *CDH1* gene (encoding E-cadherin protein) transcription and induce EMT (Batlle et al., 2000; Cano et al., 2000). Recent studies suggest that SNAIL has a much broader impact on cancer progression. In mammary epithelial cells, overexpression of SNAIL induces EMT, coupled with increased tumor-initiating properties (Mani et al., 2008). In melanoma, SNAIL promotes tumor metastasis by suppressing host immune surveillance (Kudo-Saito et al., 2009). SNAIL also cooperates with chromatin-modifying enzymes to inhibit fructose-1,6-biphosphatase (FBP1) expression, which results in increased glucose uptake, macromolecule biosynthesis, and maintenance of ATP production under hypoxic conditions (Dong et al., 2013). Given the importance of SNAIL in cancer progression, it is not surprising that many signaling pathways have been implicated in the regulation of *SNAIL* gene expression, including transforming growth factor β (TGF-β), the NOTCH and WNT pathways, reactive oxygen species, and hypoxic stress (reviewed by De Craene and Berx, 2013). A better understanding of the regulatory

Significance

SNAIL is one of the most well established master transcriptional regulators of EMT. However, a comprehensive understanding of the posttranslational regulations of these factors is lacking. We developed a high-throughput luciferase-based RNAi screening strategy to identify E3 ligase(s) targeting the SNAIL protein for ubiquitylation and degradation. We identified FBXO11 as a crucial posttranslational regulator that controls the stability of the SNAIL protein. We further uncovered that this regulation is dependent on Ser-11 phosphorylation of SNAIL by PKD1. Importantly, functional studies and clinical sample analysis established a crucial role of the PKD1-FBXO11-SNAIL axis in regulating breast cancer EMT and metastasis and indicated a potential therapeutic value of targeting this pathway.

mechanisms for SNAIL will provide critical information on how to block EMT and related processes in cancer progression.

Many transcription factors are labile proteins with short half-lives and are actively degraded through the ubiquitin-proteosome pathway. Interestingly, in many cases, E3 ligases recognize and ubiquitylate transcription factor substrates by interacting with their transcriptional activation/repressor domain. This allows the coupling of the transcriptional activity with the protein degradation process to prevent hyperactivation of important transcription factors (Muratani and Tansey, 2003). For instance, Mdm2 binds to the transactivation domain of p53, targeting it for ubiquitylation and degradation (Momand et al., 1992). Likewise, the E3 ligase FBW7 interacts with the KLF5 transactivation domain for its degradation (Liu et al., 2010; Zhao et al., 2010). Although prior studies have identified two E3 ubiquitin ligases, FBXL14 (Ppa in *Xenopus*) (Lander et al., 2011) and FBXW1 (also called β-TRCP or BTRC) (Zhou et al., 2004), responsible for SNAIL ubiquitylation and degradation, neither of them interacts with the SNAIL/Gfi-1 domain (SNAG) transcriptional repression domain of SNAIL. This leads us to suspect that there may be additional critical E3 ligase(s) that target(s) the SNAIL protein for degradation through interaction with the SNAG domain. Identifying such E3 ligase(s) and the signaling events regulating SNAIL ubiquitination will provide possible new windows for therapeutic targeting of SNAIL.

RESULTS

A Luciferase-Based Screening System for SNAIL Protein Turnover Regulation

To confirm that the SNAIL protein is posttranslationally controlled by the ubiquitin-proteosome system (UPS) in breast cancer, we first blocked protein synthesis using cycloheximide (CHX) and pulse-chased the SNAIL protein in the SUM1315 human breast cancer cell line. Indeed, SNAIL was degraded rapidly and became undetectable within 4 hr of CHX treatment (Figure 1A; Figure S1A available online). Furthermore, treatment of cells with the proteosomal inhibitor MG132 increased the stable SNAIL protein level, confirming that SNAIL is degraded through the UPS (Figure 1A; Figure S1A).

The identification of E3 ligases responsible for the degradation process of certain protein substrates has traditionally relied on serendipitous discoveries or candidate gene approaches. To identify potential E3 ligase(s) responsible for SNAIL degradation in an unbiased manner, we designed a luciferase-based small interfering RNA (siRNA) screening strategy that can be easily adapted in future discovery efforts to identify new E3 ligase-protein substrate pairs. We fused the SNAIL protein coding sequence in-frame with the *firefly luciferase* gene coding sequence (*SNAIL-Luc*) to produce the SNAIL-Luciferase fusion reporter protein (Figure 1B). This reporter allowed us to monitor the SNAIL protein stable level and its degradation dynamics by monitoring the luciferase activity. The SUM1315 cell line was first transduced with a lentiviral vector containing the *SNAIL-Luc* fusion gene and subsequently with the *Renilla*-Luciferase retrovirus to generate a dual luciferase reporter cell line with *Renilla* luciferase (R-Luc) serving as an internal control. This cell line is denoted as "SUM-SNAIL-Luc/R-Luc" to facilitate description below (Figure 1B). The SNAIL-Luc fusion protein is localized in the nucleus (Figures S1B and S1C) and has degradation dynamics similar to those of the endogenous SNAIL protein (Figures 1C and 1D and Figure S1D). In contrast, the F-Luc protein alone is very stable (Figures S1E and S1F). The luciferase activity of the SNAIL-Luc fusion protein is also readily detectable by standard firefly luciferase reporter assay and correlates with the fusion protein level (Figure 1E). Therefore, the firefly luciferase activity in this cell line reliably represents the stable level of the SNAIL-Luc protein, whereas R-Luc activity is used as an internal control for cell number and viability.

siRNA Library Screening Identified Potential E3 Ligases Targeting SNAIL Protein for Degradation

We followed the procedures outlined in Figure 1F to identify potential E3 ligase candidates for SNAIL protein. We first knocked down individual human E3 ligase by pooled siRNA (three siRNAs per gene) in SUM-SNAIL-Luc/R-Luc cells and looked for E3 ligase genes whose knockdown (KD) resulted in more than a 2-fold increase in luciferase activity of the SNAIL-Luc fusion protein (Figure 1F). The cell lysates from these positive hits were immunoblotted for SNAIL-Luc fusion protein to confirm protein stabilization. Positive E3 ligase hits were then examined by a second round of siRNA screening to confirm the results. We then cloned all positive E3 ligase genes and determined whether they can interact with SNAIL protein by coimmunoprecipitation assay (co-IP) and reciprocal co-IP for further confirmation. Only the proteins that interacted with SNAIL were considered as E3 candidates for SNAIL protein and selected for further functional testing to determine whether they can affect exogenous and endogenous SNAIL protein degradation.

The E3 siRNA library screening revealed that siRNA-mediated inhibition of multiple E3 ligase genes increased the level of SNAIL-Luc protein. Among the 554 known and predicted human E1, E2, and E3 ligases (Table S1), siRNA knockdown of more than 100 genes increased the luciferase activity by more than 2 fold (Figure 1G, top panel). This large initial pool of potential hits may include false positive candidates that do not directly regulate SNAIL protein stability. Therefore, further validation of these candidates is needed. Interestingly, in this screening, knockdown of FBXW1, a previously known E3 ligase for SNAIL (Zhou et al., 2004), increased the SNAIL-Luc protein level 2.6-fold, whereas no change was observed after knockdown of FBXL14, another SNAIL E3 identified in the *Xenopus* model (Lander et al., 2011). The cell lysates from these initial positive hits were then subjected to immunoblotting for SNAIL-Luc fusion protein (Figures S1G and S1H), for most of which an upregulation of SNAIL-Luc protein was observed. Among them, 21 E3 candidates, when knocked down individually, increased the SNAIL-Luc protein level at least 6-fold in a luciferase assay or in immunoblot analyses, the stringent criteria we set for identifying potential candidates (Table S2). A second round of siRNA screening for these 21 genes was performed, confirming that 21 siRNAs were able to consistently increase the luciferase activity and protein stable level (Figure 1G, bottom panels; Figure S1I). We cloned the cDNA coding sequences of 13 candidate genes into a lentiviral expression vector with an N-terminal HA epitope (Figure S1J). The remaining eight genes were not cloned successfully. To test the interactions between these 13 E3

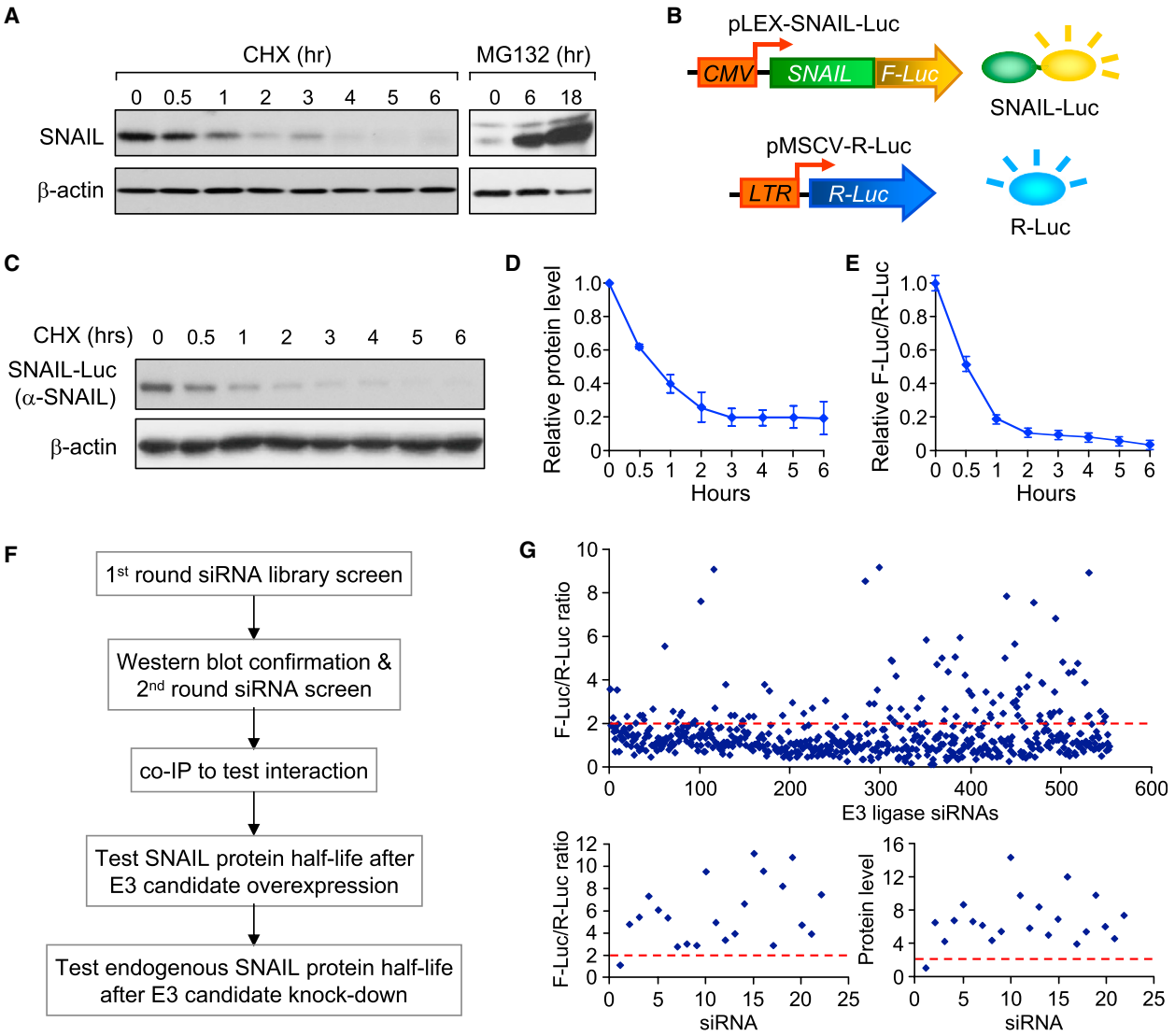

(legend on next page)

ubiquitin ligases and SNAIL, we performed a co-IP experiment to test the interactions between these E3 candidates with SNAIL. Only four E3 ligases were able to interact with SNAIL: FBXO11, SOCS3, SPSB1, and TRIM5 (Figure S1J). This result was first confirmed by repeating the co-IP experiment for these four E3 ligase proteins using HA antibody (Figure 1H) and then by reciprocal IP of the SNAIL-FLAG protein with an anti-FLAG antibody (Figure 1I). Therefore, we focused on these four E3 genes in further functional studies.

FBXO11 Is a Bona Fide E3 Ligase Targeting SNAIL Protein for Ubiquitylation and Degradation

As an initial step in functionally testing these four E3 ubiquitin ligase candidates, we cotransfected the *SNAIL-Luc* gene with individual E3 genes and examined the SNAIL-Luc protein stable level. FBXO11 expression strongly reduced the stable SNAIL-Luc protein level by up to 70% (Figures S2A and S2B). In a CHX pulse-chase analysis of SNAIL-Luc, FBXO11 accelerated SNAIL-Luc protein degradation, whereas SOCS3, SPSB1, and TRIM5 had only modest or negligible effects on SNAIL-Luc protein degradation (Figure 2A; note that, in this and other similar pulse-chase figures, Western blot images with different exposure times were used so that the basal SNAIL-Luc protein band intensity at time = 0 hr is the same across the experimental group to illustrate the differences in the kinetics of degradation).

To directly test the effect of FBXO11 on endogenous SNAIL protein degradation, we generated FBXO11-overexpressing stable cell lines using SUM1315 and the LM2 subline of MDA-MB-231 (Minn et al., 2005). In both cell lines, we observed a dramatic increase of endogenous SNAIL protein degradation (Figures S2C–S2F). Next we confirmed the interaction between endogenous SNAIL and FBXO11 proteins by co-IP experiments using MG132-treated LM2 cell lysate (Figure 2B). To further investigate whether FBXO11 functions as a bona fide E3 ligase that ubiquitylates the SNAIL protein, we cotransfected 293T cells with SNAIL-FLAG, FBXO11, and HA-ubiquitin and treated the cells with MG132 for 6 hr to prevent protein degradation before performing an ubiquitylation assay. A significant increase of polyubiquitylated SNAIL protein was observed in FBXO11-transfected cells, whereas an F-box (Skp1, Cullin, F-box [SCF] complex formation domain) deletion mutant of FBXO11 (FBXO11-ΔF) was not able to increase SNAIL ubiquitylation (Figure 2C).

Because SNAIL protein has been reported as a marker for a poor prognosis, with its high expression correlated with worse patient outcome (Moody et al., 2005), we hypothesized that E3 ligase(s) targeting SNAIL should be a marker for a good prognosis. Indeed, using the NKI295 breast cancer data set (van de Vijver et al., 2002), we found that higher *FBXO11* gene expression correlates significantly with longer metastasis-free survival (Figure 2D), whereas *SPSB1*, *SOCS3*, and *TRIM5* do not correlate with metastasis-free survival (Figure S2G).

To test the effect of reducing endogenous FBXO11 expression on SNAIL protein degradation, we used siRNAs to knock down *FBXO11* gene expression in MCF10A cells. The stable level of SNAIL protein was found to be upregulated more than 2-fold after siRNA treatment (Figure 2E, left panel, without CHX treatment). Furthermore, SNAIL protein was much more stable after FBXO11 KD in a CHX pulse-chase assay (Figure 2E). Stabilization of SNAIL after FBXO11 KD was also observed in the LM2 cell line (Figures S2H and S2I). Taken together, our results suggest that SCF-FBXO11 is a bona fide E3 ubiquitin ligase targeting SNAIL protein for ubiquitylation and degradation.

We confirmed that two previously reported E3s for SNAIL, FBXW1 and FBXL14, also interact with SNAIL, whereas other closely related F-box family members do not bind to SNAIL (Figures S2J–S2L). Interestingly, FBXW1 promoted SNAIL protein degradation, whereas FBXL14 had no effect on SNAIL stability (Figures S2M and S2N). Conversely, FBXW1 KD increased SNAIL stability, whereas no effect was observed after FBXL14 KD. Importantly, simultaneous KD of FBXO11 and FBXW1 led to increased SNAIL stabilization compared with either FBXO11 or FBXW1 KD alone (Figure 2E, right panel; Figures S2O and S2P). These results suggest that both FBXO11 and FBXW1 are capable of promoting SNAIL degradation and may function collectively to control SNAIL stability.

FBXO11 Blocks SNAIL-Induced EMT and Tumorigenesis

SNAIL has been shown to induce EMT and increases the tumor-initiating capability in nontransformed or oncogene-transformed HMLE human mammary epithelial cells (Mani et al., 2008). We tested whether FBXO11 can block SNAIL-induced EMT by transducing Neu-transformed HMLEN cells with either SNAIL alone or together with FBXO11. SNAIL expression induced strong EMT phenotypes in HMLEN cells, with loss of E-CADHERIN and upregulation of VIMENTIN and FIBRONECTIN (Figure 3A; Figures S3A and S3B). When SNAIL and FBXO11 were coexpressed in HMLEN cells, the stable level of SNAIL protein was decreased significantly compared with cells only expressing SNAIL (Figure S3A). The reduced level of SNAIL led to the reversal of the

Figure 1. A Genome-wide Functional Screen for E3 Ubiquitin Ligase(s) Targeting SNAIL Protein for Degradation

(A) In SUM1315 cells, endogenous SNAIL protein was detected by Western blot analysis after CHX (left panel) or MG132 treatment (right panel) for the indicated hours. Western blot data are quantified in Figure S1A.

(B) Illustration of the dual luciferase reporter screening system for SNAIL-targeting E3 ligases. CMV, cytomegalovirus; LTR, long terminal repeat.

(C and D) CHX pulse-chase experiment demonstrating the degradation of SNAIL-F-Luc fusion protein in SUM-SNAIL-Luc/R-Luc cells (C). Western blot data are quantified in (D). Data are presented as mean ± SEM.

(E) The degradation of SNAIL-F-Luc protein was monitored by normalized luciferase activity measurement. Data are presented as mean ± SEM.

(F) Experimental procedure flow chart for identification of the E3 ubiquitin ligase(s) targeting SNAIL protein. See text for details.

(G) Luciferase-based siRNA library screen against human E3 ligases identified multiple E3 candidates that, when knocked down in SUM-SNAIL-Luc/R-Luc cells, increased luciferase activity more than 2-fold (top panel). A second round of siRNA screening (bottom left panel) and immunoblotting (bottom right panel) was performed for confirmation of candidates.

(H and I) 293T cells were transfected according to the panel labels. The co-IP experiment was performed using either an HA antibody to pull down HA-tagged E3 ligase proteins (H) or an anti-FLAG antibody against SNAIL-FLAG protein (I).

See also Figure S1 and Tables S2 and S1.

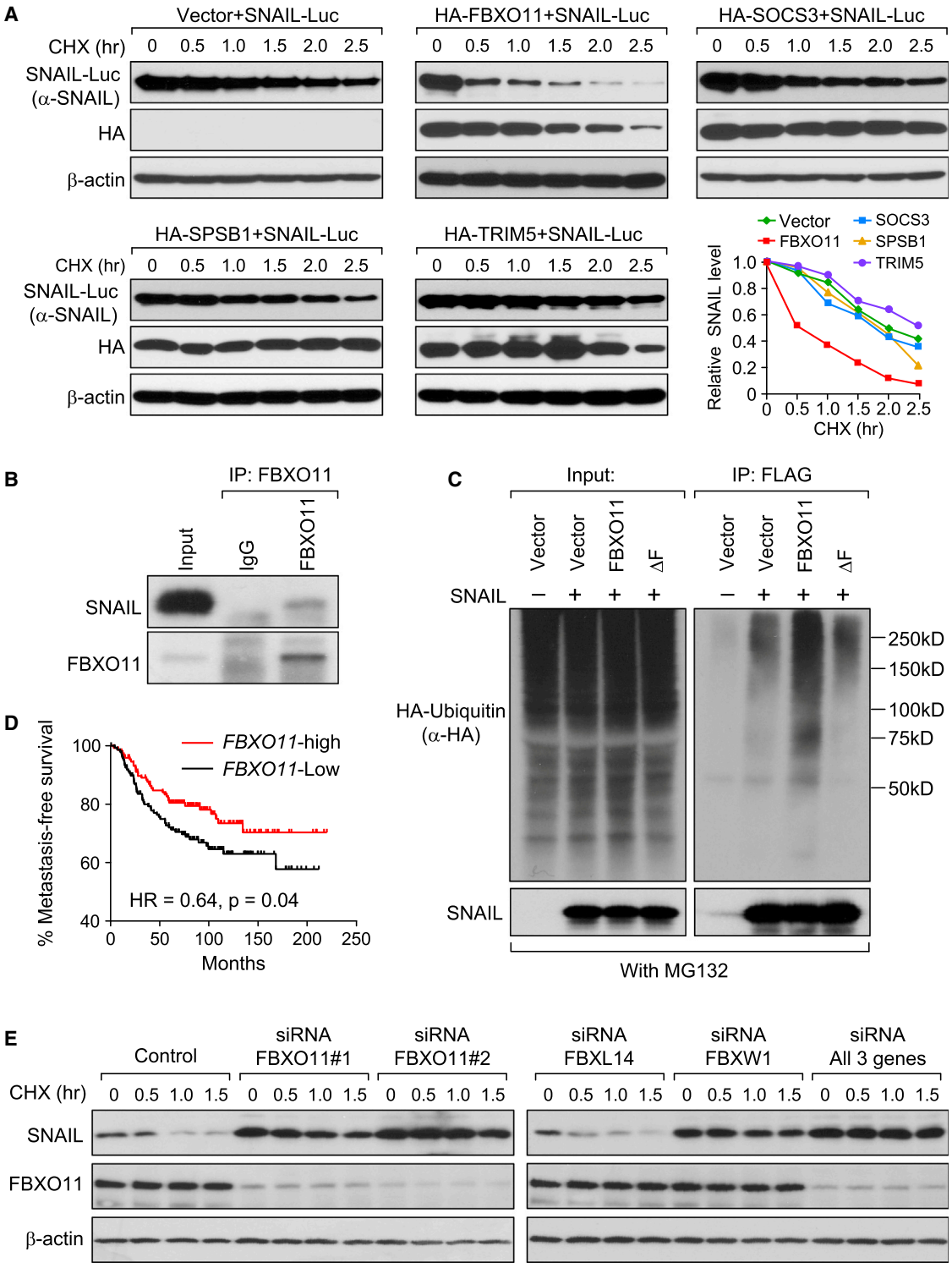

Figure 2. FBXO11 Is a Bona Fide E3 Ligase Targeting SNAIL Protein for Ubiquitination and Degradation

(A) Four E3 ligase candidates or a control pLEX-vector were cotransfected with the SNAIL-Luc plasmid into 293T cells, and a CHX pulse-chase assay was performed. Western blot data were quantified using ImageJ software.

(B) LM2 cells were treated with 10 μM MG132 for 6 hr before the cell lysate was immunoprecipitated with FBXO11 antibody or an immunoglobulin G (IgG) control and subjected to Western blot analysis.

(C) 293T cells were cotransfected with plasmids expressing HA-Ub and SNAIL-FLAG together with either a vector control, FBXO11, or the FBXO11-ΔF plasmid. Cells were treated with MG132 for 6 hr before cell lysates were immunoprecipitated using a denature IP protocol to pull down SNAIL protein, and the poly-ubiquitylated SNAIL protein was detected by anti-HA antibody.

(legend continued on next page)

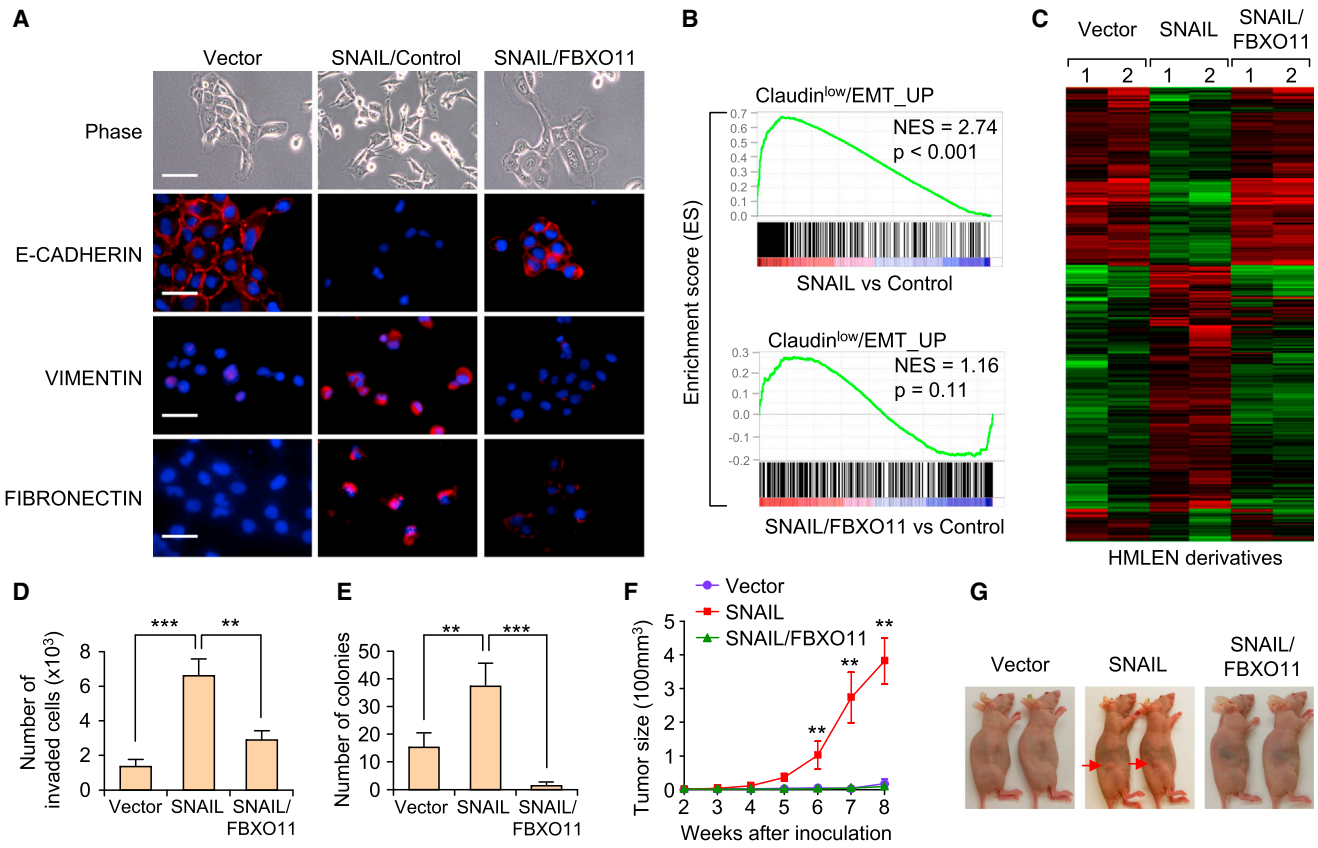

Figure 3. FBXO11 Blocks SNAIL-Induced EMT and Reduces Tumorigenesis Capability in HMLEN Cells

(A) Phase contrast and immunofluorescent (IF) images of HMLEN cells with stable overexpression of SNAIL or SNAIL together with FBXO11. Scale bar, 100 μm (phase contrast images) and 25 μm (IF images).

(B) GSEA analysis of the environment of the EMT gene signature in HMLEN cells after overexpression of SNAIL with or without FBXO11.

(C) A heatmap was generated using hierarchical clustering of the microarray data for the indicated HMLEN cell lines. The 2,327 gene probes used for clustering were those showing >2-folds expression changes upon SNAIL overexpression. The experiment was performed in duplicates.

(D) Boyden chamber invasion assay of HMLEN cells with SNAIL or SNAIL/FBXO11 overexpression. The data are shown as the mean of collected data from three triplicate wells of three independent experiments. Data are presented as mean ± SEM. $^{**}p < 0.01$, $^{***}p < 0.001$.

(E) Quantification of the colony formation assay results for the indicated HMLEN cell lines. Data are presented as mean ± SEM. $^{**}p < 0.01$, $^{***}p < 0.001$.

(F and G) 2×10^4 of the indicated HMLEN cells were injected orthotopically into nude mice (n = 8), and primary mammary tumor growth was measured weekly after injection (E). Representative tumor images are shown in (G). Data represent mean ± SD. $^{**}p < 0.01$ by two-tailed Student's t test.

See also Figure S3.

EMT phenotype in HMLEN cells, with the gain of E-CADHERIN at the cell-cell junctions and the loss of VIMENTIN and FIBRONECTIN expression (Figure 3A; Figures S3A and S3B).

To evaluate the global transcriptomic changes associated with expression of SNAIL and FBXO11, we performed gene expression microarray profiling and gene set enrichment analysis (GSEA). Using four previously published EMT/cancer stem cell-related gene signatures (see Supplemental Information), we found that these signatures were enriched in SNAIL-overexpressing cells and that such an enrichment was lost in SNAIL/FBXO11 cells (see Figure 3B using the Hennessy et al., 2009 Claudin-low/EMT signature as an example). We then generated a gene expression heatmap using a list of 2,327 genes showing >2-fold differential expression between the SNAIL-overexpressing cells and the control cells. As shown in Figure 3C, FBXO11 expression largely reversed the gene expression changes induced by SNAIL. Taken together, these results suggest that FBXO11 can block the SNAIL-induced EMT program and associated global gene expression pattern.

Because cells that undergo EMT often gain migratory and invasive capabilities, we tested the Matrigel invasion ability of these cells. As expected, SNAIL expression significantly increased the invasiveness of HMLEN cells, whereas FBXO11 expression blocked SNAIL-induced invasion (Figure 3D). HMLE

(D) Kaplan-Meier plots of metastasis-free survival of patients stratified by expression of *FBXO11*. Data were obtained from the Netherlands Cancer Institute (NKI) breast cancer data set (van de Vijver et al., 2002).

(E) MCF10A cells were transfected with indicated siRNAs, followed by the CHX pulse-chase assay. Quantification data is shown in Figure S2P.

See also Figure S2.

cells that have undergone EMT have also been reported to acquire breast cancer stem cell characteristics (Mani et al., 2008). Indeed, HMLEN-SNAIL cells showed a significant increase of the $CD44^{high}/CD24^{low}$ population, whereas FBXO11 decreased this population (Figures S3C and S3D). In line with the population shift, HMLEN-SNAIL showed increased colony formation efficiency, whereas FBXO11 suppressed SNAIL-induced colony formation (Figure 3E; Figure S3E). To further test the effect of FBXO11 on tumor initiation, we injected 20,000 tumor cells orthotopically into the mammary fat pads of nude mice. HMLEN cells had minimal tumor forming capability. However, significant formation of primary tumors can be observed 8 weeks after inoculation of SNAIL-overexpressing HMLEN cells. Again, FBXO11 completely blocked SNAIL-induced tumor initiation (Figures 3F and 3G). In aggregate, our results demonstrate a prominent effect of FBXO11 in inhibiting SNAIL-induced EMT and tumorigenesis in the HMLEN model, and this effect is likely due to FBXO11-mediated ubiquitylation and degradation of SNAIL protein.

FBXO11 Blocks SNAIL-Induced EMT and Lung Metastasis In Vivo

To test the functional impact of FBXO11 on SNAIL-induced EMT in breast cancer metastasis, we decided to use the epithelial-like 4T1 and EpRas mouse mammary tumor cell lines, which are sensitive to Snail-induced EMT and have much more robust primary tumor growth capability than HMLEN. As expected, FBXO11 expression accelerated SNAIL degradation in 4T1 cells (Figure S4A). SNAIL overexpression in the epithelial-like 4T1 and EpRas cell lines induced an EMT-like phenotype, including the reduction of E-cadherin and upregulation of N-cadherin or Vimentin expression at the both mRNA and protein levels (Figures 4A and 4B; Figures S4B–S4D). Strikingly, FBXO11 expression blocked SNAIL-induced EMT in both cell lines. Gene expression profiling revealed that the enrichment of EMT gene signatures in SNAIL-overexpressing cells was reversed by FBXO11 overexpression (Figure 4C). Likewise, overexpression of FBXO11 suppressed the SNAIL expression signature in 4T1 cells (Figure 4D). Consistent with cellular phenotype and gene expression changes, the increased invasive capability of SNAIL-overexpressing 4T1 cells was inhibited by FBXO11 (Figure S4E). Importantly, although SNAIL overexpression did not affect primary tumor growth when 10^5 tumor cells were injected orthotopically (Figure S4F), its expression significantly increased spontaneous lung metastasis in vivo (Figures 4E and 4F). The lung metastasis-promoting effect of SNAIL was reversed after FBXO11 overexpression (Figures 4E and 4F), again without any significant alteration in the primary tumor growth rate (Figures S4F and S4G).

To complement the findings obtained by using SNAIL and FBXO11-overexpressing cells, we knocked down endogenous Fbxo11 in 4T1 cells by short hairpin RNAs (Figure 5A). Western blot analysis revealed a 5-fold upregulation of Snail protein after stable knockdown of Fbxo11 (Figure 5B). Fbxo11 KD in 4T1 cells induced EMT-like cellular changes, including reduction of E-cadherin and increase of Vimentin at the mRNA (Figure 5A) and protein levels by Western blot analysis and immunofluorescence analyses (Figures 5B and 5C). Importantly, Fbxo11 KD significantly increased lung metastasis (Figures 5D and 5E), despite no difference in primary tumor growth (data not shown). Western blot analysis of primary tumors confirmed that Snail expression was upregulated and that E-cadherin expression was reduced in Fbxo11 KD tumors (Figure S5A), consistent with an in vitro analysis. Fbxo11 KD and Snail upregulation were also maintained in lung metastasis nodules (Figure S5B). These results indicate that FBXO11 inhibits metastasis by promoting the ubiquitylation and degradation of the EMT-inducing SNAIL protein.

Phosphorylation of Ser-11 on the SNAG Domain Is Essential for SNAIL to Be Recognized by FBXO11

FBXO11 belongs to a large group of the F-box protein superfamily. These proteins usually exert their E3 ligase function by forming a four-subunit functional complex with Cullin, Skp, and Rbx proteins (SCF complex), with F-box proteins as a substrate recognition component. Interestingly, F-Box proteins generally recognize the protein substrate when they are phosphorylated (Cardozo and Pagano, 2004). Therefore, it is plausible that SNAIL protein also needs to be phosphorylated before being recognized by FBXO11. To investigate this, we performed a modified co-IP experiment in which cell lysate from 293T cells transfected with SNAIL and FBXO11 was treated with or without alkaline phosphatase (calf intestinal phosphatase [CIP]) to remove protein phosphorylation before IP. SNAIL was pulled down together with FBXO11 protein, and this interaction was completely disrupted by CIP treatment (Figure 6A), suggesting that phosphorylation modification of either or both SNAIL and FBXO11 might be critical for the SNAIL-FBXO11 protein interaction. To identify the potential region within the SNAIL protein that is phosphorylated and responsible for SNAIL-FBXO11 interaction, we generated several SNAIL truncation mutations and performed the co-IP experiment. Interestingly, only two truncation mutants, ΔSNAG and Δ194 (both lacking the first 20 amino acid SNAG domain on the SNAIL protein) (Figure 6B), lost the ability to interact with FBXO11 (Figure 6C). Immunofluorescence analysis indicated that ΔSNAG remained localized in the nucleus, suggesting that loss of interaction between ΔSNAG and FBXO11 was not due to localization change (Figure S7A). Therefore, the SNAG domain of SNAIL protein is critical for its interaction with FBXO11.

As recent literature suggests, there are at least five kinases that phosphorylate SNAIL protein at distinct amino acids and fine-tunes the functions of SNAIL differentially (Bastea et al., 2012; Du et al., 2010; Eiseler et al., 2012; Pon et al., 2008; Yang et al., 2005; Zhang et al., 2012a; Zhou et al., 2004). Phosphorylation of the Ser-11 site by protein kinase D1 (PKD1, also known as PKCμ) lies within the domain that we identified to be responsible for SNAIL-FBXO11 interaction. Interestingly, aberrant upregulation of PKD1 has been suggested to block SNAIL-induced EMT and anchorage-independent growth (Bastea et al., 2012; Du et al., 2010; Eiseler et al., 2012). Therefore, we tested whether the PKD1 consensus phosphorylation sequence LXRXXS in the SNAG domain is essential for SNAIL-FBXO11 interaction. We generated L6A-SNAIL, R8A-SNAIL, and S11A-SNAIL alanine scanning mutants in the PKD1 consensus sequence and found that none of these mutants could interact with FBXO11 anymore (Figures S6A and S6B). Importantly, they also became stabilized compared with wild-type SNAIL protein (Figure S6C). We further generated two additional mutants in Ser11, SNAIL-S11E and SNAIL-S11V, to mimic and disrupt the phosphorylation of the SNAIL protein at Ser-11,

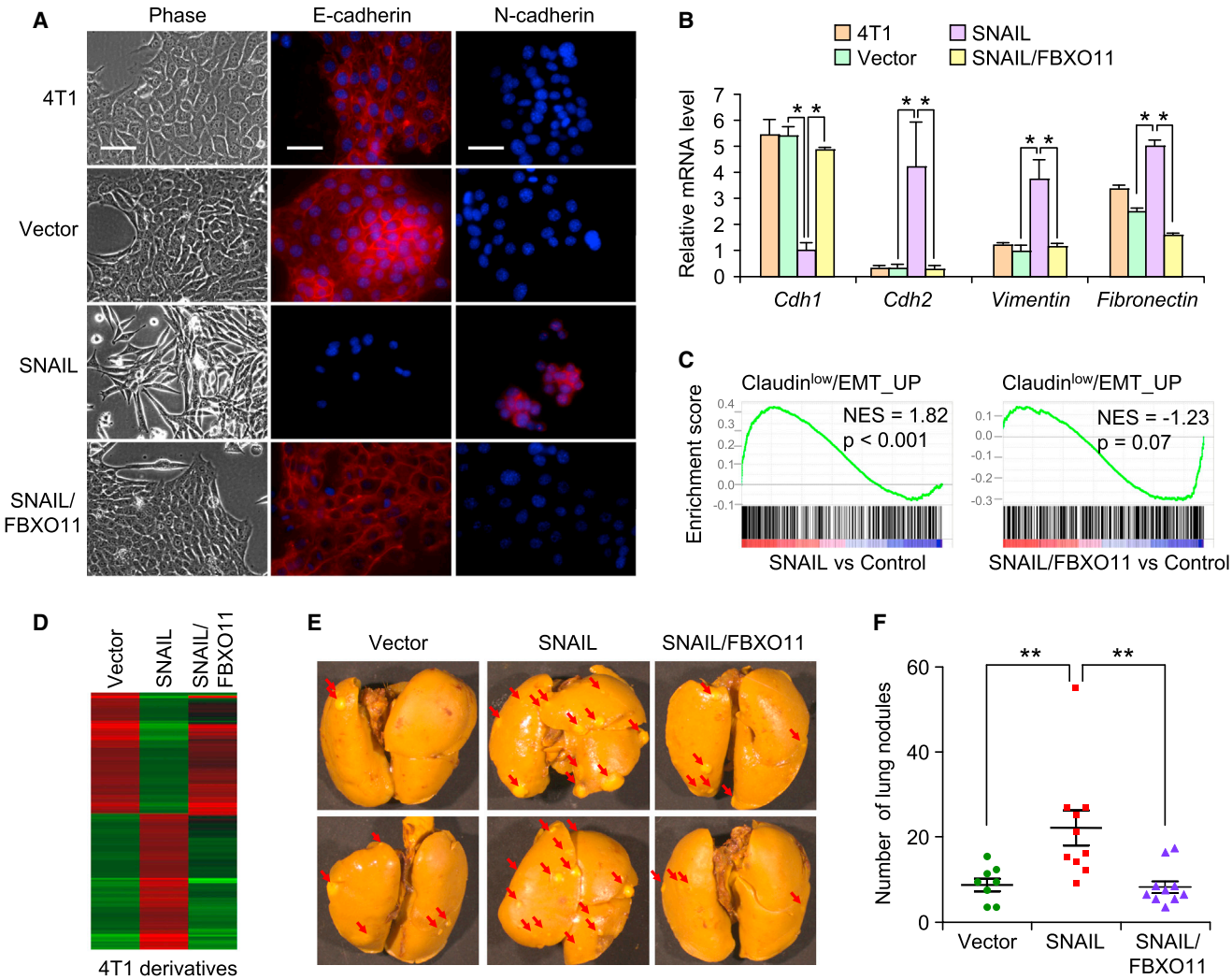

Figure 4. FBXO11 Blocked SNAIL-Induced EMT and Metastasis in the 4T1 Breast Cancer Cell Line

(A) Phase contrast and IF images for 4T1 cells transduced with the indicated lentiviruses. SNAIL induced a strong EMT program in 4T1 cells with downregulation of E-cadherin and upregulation of N-cadherin expression, whereas FBXO11 blocked SNAIL-induced EMT. Scale bars, 25 μm.

(B) Quantitative RT-PCR (qRT-PCR) analysis of EMT marker mRNAs in the indicated 4T1 cell lines. Results were normalized to the *GAPDH* mRNA level. Data represent mean ± SEM. *$p < 0.05$ by Student's t test.

(C) A GSEA analysis demonstrated that FBXO11 expression inhibited the SNAIL-induced EMT gene signature in 4T1 cells.

(D) A heatmap was generated using hierarchical clustering. The 1,400 gene probes used for clustering were those showing >2-fold expression changes in SNAIL-overexpressing cells.

(E) 10^5 cells were injected orthotopically into BALB/c mice (n = 10). The mice were sacrificed 3 weeks later. Representative lung metastasis nodule images are presented.

(F) Numbers of lung metastasis lesions of mice injected with the indicated 4T1 cell lines. **$p < 0.01$ by Mann-Whitney U test.

See also Figure S4.

respectively. The phosphorylation-disrupting S11V mutant completely lost the interaction with FBXO11 protein, whereas the phosphorylation-mimicking mutant S11E still interacted with FBXO11 (Figure 6D). Previous literature suggests that GSK-3β-dependent phosphorylation on SNAIL protein is critical for its recognition by FBXW1, another E3 ligase targeting SNAIL protein (Zhou et al., 2004). We acquired several SNAIL mutants, including the 6SA mutant, which can no longer be phosphorylated by GSK-3β, and performed a co-IP experiment with FBXO11. Our results demonstrated that these mutants did not disrupt the interaction between SNAIL and FBXO11 protein (Figure S6D). Therefore, although both FBXO11 and FBXW1 can destabilize SNAIL through UPS, distinct protein kinases are involved in producing different phosphorylated SNAIL proteins for recognition by these E3s.

To further test the effects of these mutations on SNAIL protein degradation, we transfected these mutants either alone or together with wild-type FBXO11 or FBXO11-ΔF expression vectors into 293T cells and performed the CHX pulse-chase experiment. In the absence of exogenous FBXO11, SNAIL-S11E

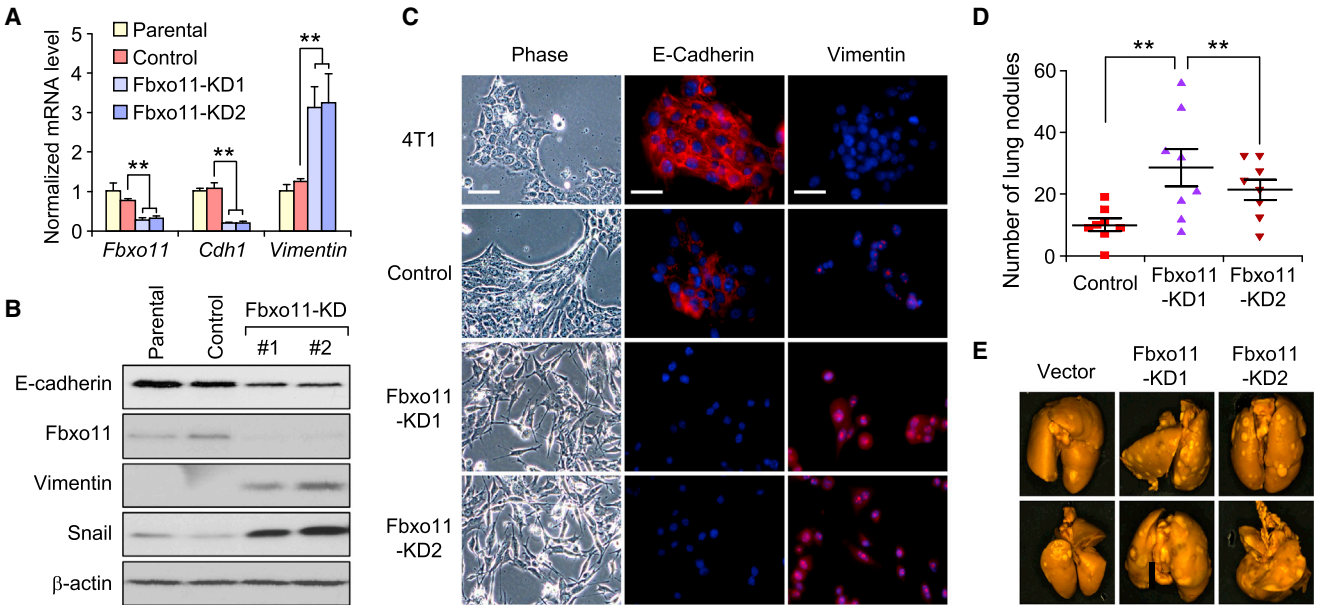

Figure 5. Knockdown of Endogenous FBXO11 Promotes Breast Cancer Metastasis

(A) Real-time PCR analysis of *Fbxo11*, *Cdh1*, and *Vimentin* expression in the parental and control 4T1 cell line and two Fbxo11-KD cell lines. Data represent mean ± SD. **$p < 0.01$ by two-tailed Student's t test.

(B) Western blot analysis of Snail, E-cadherin, and Vimentin expression in the indicated 4T1 cell lines.

(C) Phase contrast images and immunofluorescent images of EMT markers in the indicated 4T1 cell lines. Scale bars, 25 μm.

(D) 10^5 tumor cells from various 4T1 cell lines were injected orthotopically into BALB/c mice, and primary tumors were removed 10 days later. Lung metastasis nodules were counted after sacrificing the mice at 38 days postinjection. **$p < 0.01$ by Mann-Whitney U test.

(E) Representative lung metastasis nodule images.

See also Figure S5.

degraded much faster than wild-type (WT) SNAIL protein, whereas SNAIL-S11V protein was stabilized (Figure 6E and 6F). In the presence of exogenous FBXO11, the stable level of SNAIL protein was significantly lower than that of the S11V-SNAIL mutant (Figure 6G). In the CHX pulse-chase experiment, SNAIL protein turnover was accelerated by cotransfection with FBXO11 but not the FBXO11-ΔF mutant lacking the SCF complex formation domain. As expected, SNAIL-S11V was more stable compared with wild-type SNAIL protein, even in the presence of FBXO11 (Figures 6H and 6I). Taken together, our results suggest that Ser-11 is the critical amino acid for SNAIL-FBXO11 interaction.

PKD1-Dependent Phosphorylation of Ser-11 Is Critical for SNAIL Degradation

To directly test whether Ser-11 is phosphorylated by PKD1 in our system, we cotransfected 293T cells with SNAIL-FLAG, HA-FBXO11, and different wild-type or mutant PKD1 plasmids. In one set of cell lysates, we first performed IP with an anti-FLAG antibody to pull down SNAIL protein and examined the Ser-11 phosphorylation status by an antibody that specifically recognizes p-Ser-11-SNAIL. SNAIL protein presented a very strong phosphorylation band at the correct size, whereas PKD1 inhibitor CID755673 treatment resulted in a loss of this phosphorylation band. PKD1 dominant-negative mutant (PKD1-KW), but not the wild-type PKD1, also almost completely abolished SNAIL protein phosphorylation (Figure 7A). In the remaining set of cell lysates, we performed co-IP experiments with HA antibody to pull down FBXO11 protein. The PKD1 inhibitor, as well as the dominant-negative PKD1-KW mutant, disrupted the interaction between SNAIL and FBXO11 protein (Figure 7B) and stabilized SNAIL protein in the CHX pulse-chase experiment (Figure 7C; Figure S7A) without changing the localization of SNAIL (Figure S7B). Consistent with these results, PKD1 inhibitor reduced polyubiquitylated SNAIL protein bands compared with the control (Figure 7D). Importantly, both p-Ser-11-SNAIL and FBXO11 localized in the nucleus, based on immunofluorescent staining (Figure S7C), suggesting that PKD1-dependent targeting of SNAIL by FBXO11 may occur in the nucleus.

We further investigated the role of endogenous PKD1 in regulating SNAIL protein stability. When we knocked down PKD1 expression by siRNAs (Figure S7D), we observed a significant decrease in the Ser-11 phosphorylation level, loss of interaction between SNAIL and FBXO11 (Figure 7E), and stabilization of the endogenous SNAIL protein (Figure 7F; Figure S7E). Previous reports demonstrated that RhoA is a physiological activator for PKD1 kinase (Eiseler et al., 2009). Therefore, we used a constitutively activated (CA) RhoA and a RhoA inhibitor, Exoenzyme C3 transferase protein (C3), to test their effects on SNAIL protein degradation. We first confirmed the PKD1 activation status by probing p-PKD1-744/748 in PKD1 pull-down samples (IP with HA antibody) (Figure S7F). SNAIL and FBXO11 interaction was also diminished significantly by the RhoA inhibitor (Figure S7G). Consistently, SNAIL was stabilized after RhoA inhibition by C3, whereas SNAIL degradation was accelerated in cells cotransfected with the RhoA-CA mutant (Figure 7G; Figure S7H). Taken

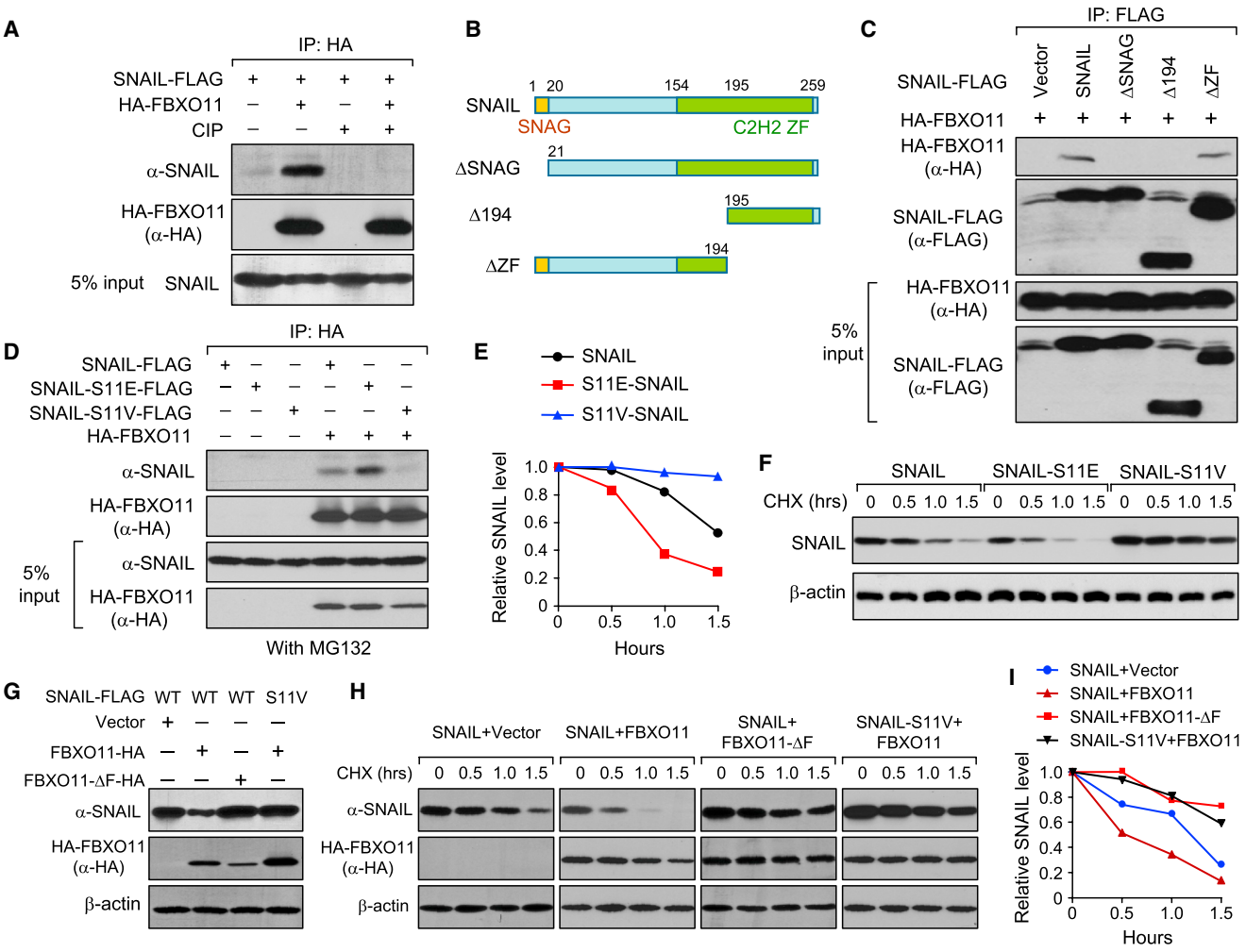

Figure 6. Ser-11 in the SNAG Domain of SNAIL Is Responsible For Interaction with FBXO11

(A) 293T cells were transfected with SNAIL-FLAG and HA-FBXO11 for 2 days. Cell lysates were collected and treated either with or without CIP for 1 hr before subjected to a co-IP experiment.

(B) Schematic of the SNAIL protein structure and the deletion mutation constructs generated to map out the interaction domain for SNAIL-FBXO11 interaction.

(C) Wild-type FLAG-tagged SNAIL and SNAIL truncation mutants were cotransfected with HA-FBXO11 into 293T cells, and cell lysates were collected for the co-IP experiment using anti-FLAG antibody.

(D) Wild-type SNAIL and SNAIL-S11E and SNAIL-S11V single amino acid mutants were cotransfected with HA-FBXO11 into 293T cells, and cell lysates were collected for the co-IP experiment using anti-HA antibody.

(E) CHX pulse-chase assay for wild-type SNAIL, SNAIL-S11E, and SNAIL-S11V in the absence of exogenously expressed FBXO11 in 293T cells. Data were quantified using ImageJ software.

(F) Western blot images of the experiments in (E).

(G) 293T cells were transfected with the indicated expression plasmids, and cell lysates were collected for immunoblotting two days after transfection.

(H and I) 293T stable cells expressing corresponding wild-type SNAIL or mutant SNAIL were transfected with the indicated FBXO11 expression plasmids (H). A pulse-chase assay was performed 2 days later. Data were quantified in (I) using ImageJ software.

See also Figure S6.

together, our results demonstrate that SNAIL is phosphorylated by PKD1 at Ser-11, which promotes the interaction, ubiquitylation, and degradation of SNAIL protein.

Previous results have demonstrated that WT SNAIL failed to induce EMT in MCF7 cells, possibly because of its rapid turnover rate and low stable protein level in this cell line (Zhou et al., 2004). On the other hand, the SNAIL-6SA mutant, with disruption of the GSK-3β phosphorylation sites (the binding site for FBXW1), was able to induce EMT in MCF7 cells. Because the SNAIL-S11V mutant disrupted the PKD1 phosphorylation site and also stabilized SNAIL protein, we sought to determine whether the S11V mutant is also able to induce EMT in MCF7 cells. Similar to what has been reported before (Zhou et al., 2004), although SNAIL failed to induce complete EMT in MCF7 cells, the 6SA mutant induced strong EMT phenotypes in MCF7 cells (Figure 7H). The S11V mutant and the double S11V/6SA mutants also induced a significant EMT program in MCF7 cells (Figure 7H). Immunofluorescent staining revealed a decrease of

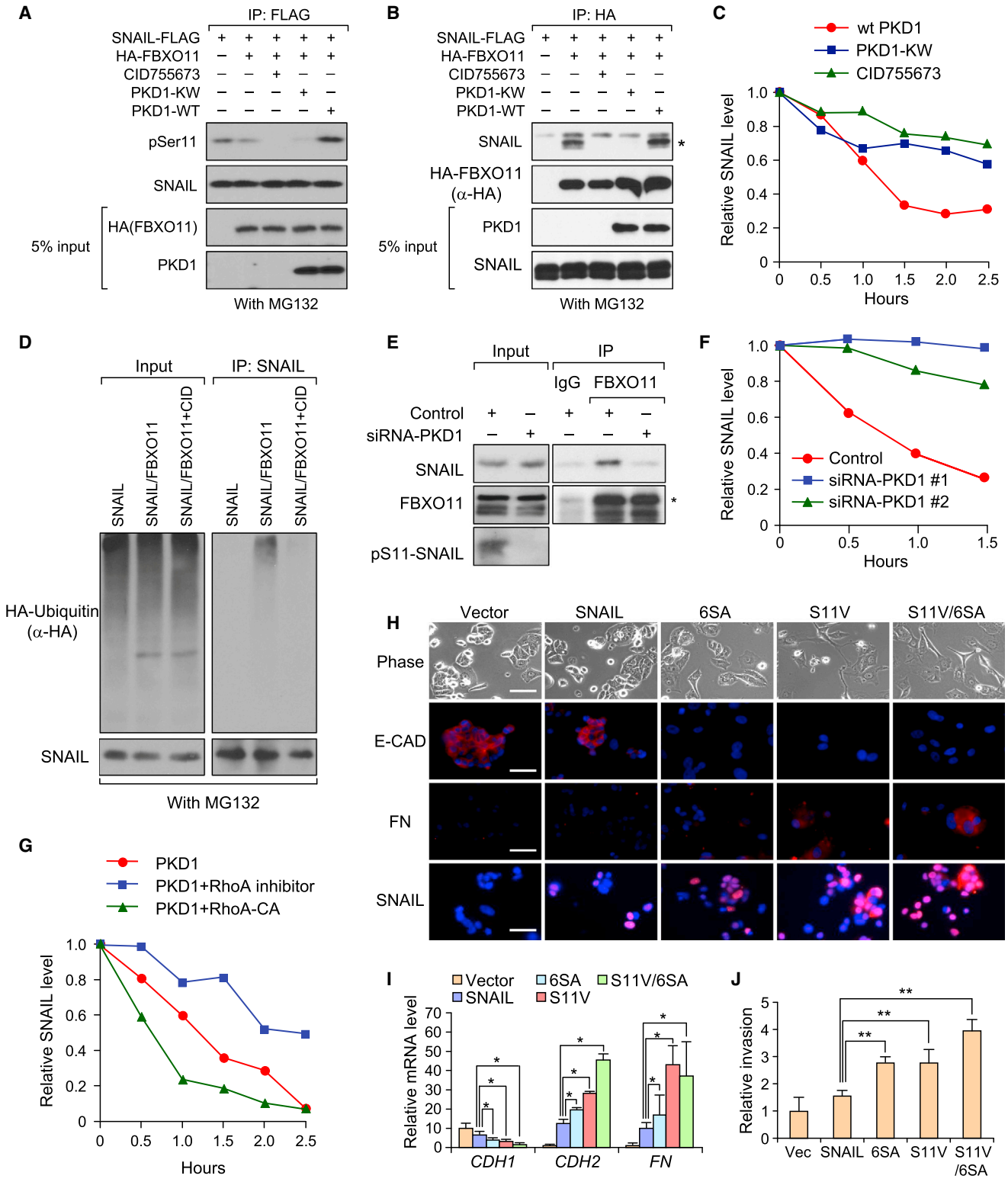

Figure 7. PKD1-Dependent Phosphorylation of SNAIL Ser-11 Is Critical for SNAIL Protein Degradation

(A) Detection of Ser11 phosphorylation of immunoprecipitated SNAIL protein when SNAIL was cotransfected with the indicated plasmids or treated with the PKD1 inhibitor CID755673 in 293T cells. Cells were treated with MG132 for 6 hr before co-IP experiments.

(B) 293T cells were transfected or treated similarly as in (A) and then lysed, and a co-IP experiment was performed using anti-HA antibody. Cells were treated with MG132 for 6 hr before co-IP experiments.

(legend continued on next page)

E-CADHERIN at the cell membrane and an increase of FIBRONECTIN in 6SA-, S11V-, and S11V/6SA-transduced MCF7 cells but not in control or wild-type SNAIL-transduced MCF7 cells (Figure 7H). Furthermore, although SNAIL was able to reduce *CDH1* expression and increase *CDH2* and *FN* levels, these changes were minimal compared with 6SA-, S11V-, and S11V/6SA-induced changes. 6SA and S11V seem to have similar effects on repression of *CDH1* expression and induction of *CDH2*/*FN* expression, whereas combining these two mutants presented the strongest EMT phenotype, based on mRNA profiles (Figure 7I). To functionally test the effect of these mutants on tumor invasion ability, we performed a Matrigel invasion assay and revealed that the S11V-SNAIL and 6SA-SNAIL mutants induced a much stronger invasive capability compared with WT SNAIL or a vector control (Figure 7J). In aggregate, our results demonstrate that PKD1 is responsible for phosphorylation of Ser-11 on SNAIL protein and that this phosphorylation promotes SNAIL protein ubiquitylation and degradation.

Negative Correlation of PKD1 and FBXO11 with SNAIL in Clinical Breast Cancer Samples

We used immunohistochemistry (IHC) staining to examine the SNAIL protein expression level with the invasive property in 136 breast tumor samples collected at Sun Yat-Sen University Cancer Center. Nuclear SNAIL protein expression correlates positively with lymph node invasion (Figure 8A; Pearson χ^2 = 4.9, p = 0.026). Based on our finding that PKD1 phosphorylation promotes SNAIL degradation, we next investigated the prognosis value of PKD1. Consistent with its role in promoting SNAIL protein degradation, a higher *PKD1* expression level correlates with longer relapse-free survival (Figure 8B; hazard ratio = 0.79, p < 0.001) in a large public clinical microarray database of breast tumors from 1,354 patients (Győrffy et al., 2010). Next, we tested the possible correlation between activated PKD1 (pY95-PKD1 antibody staining) and p-Ser-11 SNAIL protein levels using a tissue microarray containing 100 breast cancer patient samples. Consistent with a previous report (Bastea et al., 2012), activated PKD1 expression correlates positively with p-Ser-11 SNAIL protein expression (Figures 8C and 8D; χ^2 = 10.0, p = 0.0016). Finally, we tested the correlation between FBXO11 and SNAIL expression in the same breast tumor samples and observed a strong negative correlation between FBXO11 and nuclear SNAIL expression because more than 70% of FBXO11-low samples have a high SNAIL level (Figures 8E and 8F; χ^2 = 7.49, p = 0.0062).

In conclusion, our study reveals a functionally important post-translational control mechanism of the EMT master regulator SNAIL. Our results suggest a model in which SNAIL protein is phosphorylated by PKD1 kinase at the Ser-11 residue. Phosphorylated SNAIL protein is then recognized and polyubiquitylated by the SCF-FBXO11 E3 ligase complex for proteosomal degradation, thereby limiting its ability to induce EMT, tumor initiation, and metastasis (Figure 8G).

DISCUSSION

SNAIL is a conserved transcription factor that plays an essential role in EMT during cancer metastasis. Recent discoveries also revealed that SNAIL has a much broader effect on cancer progression, linking the *SNAIL* gene not only to EMT but also to cancer stem cell properties (Mani et al., 2008), immune evasion (Kudo-Saito et al., 2009), cancer metabolism (Dong et al., 2013), and breast cancer relapse (Moody et al., 2005). Given these important roles, a better understanding of the regulatory mechanisms of the SNAIL protein level will provide additional avenues to inhibit SNAIL-induced tumor malignancy in breast cancer.

Previous results have demonstrated that SNAIL is a labile protein with a very short half-life (Zhou et al., 2004). Although E3 ligases often recognize their transcriptional factor substrates by binding to their transcriptional regulatory domains, neither one of the two previously identified E3 ligases for SNAIL, FBXW1/β-TRCP, and FBXL14 interacts with the SNAG transcriptional repression domain of SNAIL (Lander et al., 2011; Zhou et al., 2004), leading us to suspect that there exist(s) additional E3 ligase(s) targeting the SNAG domain under the control of important kinase signaling pathways. Conventionally, identifying such E3 ligases is a time-consuming and often serendipitous process. Proteomic analyses have been used to identify protein substrates for certain E3 ligases (Emanuele et al., 2011). However, this method is not suitable to search for E3 ligases that can degrade a specific protein substrate of interest. We developed a luciferase-based screening method to discover candidate E3 ligases for a specific protein substrate (SNAIL). It is worth

(C) In 293T cells stably transfected with SNAIL, SNAIL protein turnover rates were determined by CHX pulse-chase assays after cells were transfected with FBXO11 together with the indicated plasmids or the inhibitor CID755673. The Western blot images in Figure S8A were quantified using Image J software.
(D) 293T cells were transfected with the indicated plasmids. Cells were treated with DMSO or the PKD1 kinase inhibitor CID755673 before lysing in denature lysis buffer. Cell lysates were subjected to denature IP with SNAIL antibody. Polyubiquitylated SNAIL protein was visualized by HA antibody blotting against HA-ubiquitin. Cells were treated with MG132 for 6 hr before co-IP experiments.
(E) MCF10A cells were treated with either 10 nM control or PKD1-targeting siRNA before being subjected to co-IP and Western blot analysis using the indicated antibodies. Cells were treated with MG132 for 6 hr before co-IP experiments.
(F) MCF10A cells were transfected with control or two PKD1 siRNAs. Two days later, endogenous SNAIL degradation was determined by CHX pulse-chase assay. The Western blot images in Figure S7E were quantified using ImageJ software.
(G) The 293T-SNAIL stable cell line was transfected with HA-PKD1 together with either vector or GST-tagged, constitutively active RhoA-CA, and a CHX pulse-chase assay was performed for SNAIL. The Western blot images in Figure S7H were quantified using ImageJ software.
(H) Representative phase contrast images and immunofluorescent images of MCF7 cells stably expressing SNAIL or SNAIL mutants. Scale bars, 25 μm. E-CAD, E-cadherin; FN, Fibronectin.
(I) qRT-PCR was performed for *CDH1*, *CDH2*, *VIM*, and *FN* in the indicated MCF7 stable cell lines. Data represent mean ± SD. *p < 0.05 by two-tailed Student's t test.
(J) Boyden chamber invasion assay of MCF7 cells stably expressing SNAIL or SNAIL stabilization mutants. Data represent mean ± SD. **p < 0.01 by Student's t test. Vec, vector.
See also Figure S7.

A

	SNAIL-hi	SNAIL-lo	Total
LN+	40	27	67
LN-	28	41	69
Total	68	68	136

χ^2=4.9, p = 0.026

B

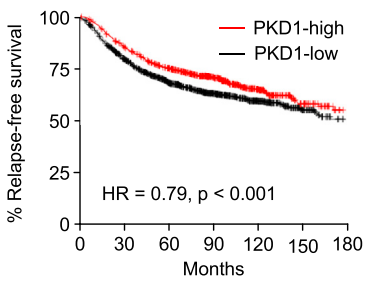

C

	pS11-lo	pS11-hi	Total
pY95-lo	31	14	45
pY95-hi	18	34	52
Total	49	48	97

χ^2=10.0, p = 0.0016

D

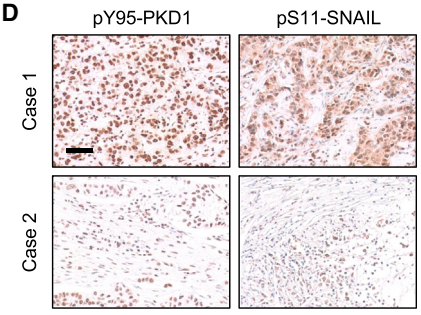

E

	SNAIL-lo	SNAIL-hi	Total
FBXO11-lo	13	37	50
FBXO11-hi	26	21	47
Total	39	58	97

χ^2=7.49, p = 0.0062

F

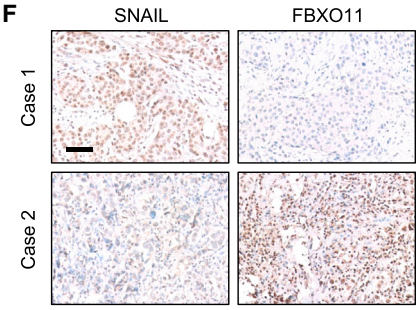

G

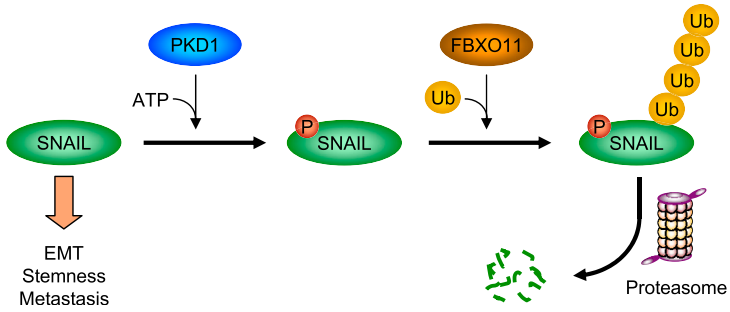

Figure 8. The SNAIL Protein Expression Level Correlates Positively with Lymph Node Invasion and Negatively with the FBXO11 Expression Level in Breast Cancer Patients

(A) Correlation study of the SNAIL expression level with lymph node invasion in 136 breast tumor specimens. SNAIL-lo, SNAIL IHC staining lower than median; SNAIL-hi, SNAIL IHC staining higher than median; LN−, without lymph node invasion; LN+, with lymph node invasion. χ^2 = 4.9, p = 0.026 by χ^2 test.

(B) Kaplan-Meier plots of distant relapse-free survival of patients, stratified by expression of *PKD1*. Data obtained from the Kaplan-Meier plotter database (Győrffy et al., 2010).

(C) Correlation study of activated PKD1 (pY95-PKD1) and S11-SNAIL in a breast tumor tissue microarray (US Biomax BC081120). χ^2 = 10.0, p = 0.0016 by χ^2 test.

(D) Representative IHC images of pY95-PKD1 and p-S11-SNAIL in breast tumors. Scale bars, 100 μm.

(E) Correlation study of SNAIL and FBXO11 in the same breast tumor tissue microarray. χ^2 = 7.49, p = 0.0062 by χ^2 test.

(F) Representative IHC images of SNAIL and FBXO11 in breast tumors. Scale bars, 100 μm.

(G) Schematic of PKD1-dependent SNAIL protein ubiquitylation and degradation by FBXO11. SNAIL protein is first phosphorylated by PKD1 kinase at Ser-11 before it can be recognized and ubiquitylated by the SCF-FBXO11 E3 ligase complex. Polyubiquitylated SNAIL protein is then degraded through the 26S proteosomal degradation pathway.

noting that other candidate SNAIL-targeting E3s identified in our initial screen, including SOCS3, SPSB1, and TRIM5, can interact directly with SNAIL and that the knockdown of these E3s increased the steady-state level of SNAIL. However, overexpression of these three E3s did not accelerate SNAIL degradation. It is possible that these E3s are already expressed at relative high levels in 293T cells and that further overexpression of these three E3 ligases will not further enhance their activity. The other potential explanation is the off-target effect of siRNA knockdown. For these reasons, we only consider an E3 as a true candidate when it has strong effects on SNAIL protein degradation in both knockdown and overexpression experiments. Overall, our study serves as the proof of principle for adopting such a screening and validation strategy to effectively identify other E3 ligase-substrate pairs.

Functionally, FBXO11 blocks SNAIL-induced EMT in HMLEN cells, a commonly used breast cancer EMT model, by promoting SNAIL protein degradation. Although HMLEN-SNAIL cells become more mesenchymal-like with enhanced tumor-initiating properties, FBXO11 coexpression completely reverses these phenotypes. FBXO11 also prevents SNAIL-induced EMT and in vivo metastasis in the 4T1 and EpRas mammary tumor cell lines by ubiquitylating and degrading SNAIL protein. Knockdown of endogenous Fbxo11 also stabilizes SNAIL protein, induces EMT in 4T1 cells, and promotes lung metastasis. In line with its role as a negative regulator of the prometastatic protein SNAIL, higher *FBXO11* expression correlates with longer metastasis-free survival in breast cancer patients. In our preliminary analysis, we did not find any correlation of *FBXO11* expression with the breast cancer subtype using the publically available NKI295 data set, which has a limited sample size. However, future studies using larger data sets are needed to further analyze whether FBXO11 is correlated negatively with the Claudin-low subtype, in which the gene expression signature

of tumor samples resembles that of normal and cancerous stem cells of the mammary gland.

Previous publications identified five kinases that can phosphorylate SNAIL protein. In our search, we found that PKD1-dependent phosphorylation of Serine-11 on the SNAG domain is the rate-limiting step for FBXO11-mediated SNAIL protein ubiquitylation and degradation. Mutation of the consensus PKD1 phosphorylation site on SNAIL, particularly Ser-11, blocks its phosphorylation by PKD1 and disrupts the interaction of SNAIL with FBXO11. Stabilized SNAIL-S11V protein promotes EMT in MCF7 breast cancer cell lines, whereas the wild-type SNAIL fails to do so. The SNAIL-FBXO11 complex is likely formed in the nucleus, where both p-Ser-11-SNAIL and FBXO11 are detected. Although p-Ser-11-SNAIL is most abundant in the nucleus, we cannot rule out the possibility that PKD1-dependent phosphorylation can still occur in the cytoplasm because many transcriptional factors are shuttling constantly between the nucleus and the cytoplasm.

Our result is also consistent with previously established functional role of PKD1 during EMT process. PKD1 has been reported to maintain the epithelial phenotype and inhibit EMT by phosphorylation of SNAIL protein. PKD1 phosphorylates Ser-11 on SNAIL, causing the repression of E-cadherin expression by triggering SNAIL nuclear export (Du et al., 2010) or by forming an inactive DNA/SNAI1 complex that shows decreased interaction with its corepressor Ajuba (Bastea et al., 2012). Our findings demonstrate that the phosphorylation at Ser-11 by PKD1 serves as another, previously unknown distinct functional role in regulating SNAIL-induced EMT and metastasis by promoting SNAIL protein ubiquitylation and degradation. Our analysis reveals that FBXO11 interacts with the PKD1-phosphorylated SNAG transcription repressor domain, suggesting that FBXO11 is indeed an important "classical" E3 ligase targeting SNAIL protein for degradation by coupling the transcriptional activity with the degradation process. Clinical sample analysis also confirms a positive correlation of activated PKD1 and p-Ser-11 SNAIL expression. Importantly, we also observed a strong negative correlation of SNAIL protein and FBXO11 protein expression in breast cancer patients. Interestingly, it has been shown recently that the PKD1 level was regulated at the epigenetic level (Borges et al., 2013). The *PKD1* promoter is highly methylated, leading to a reduced PKD1 level in metastatic breast cancer cells compared with nonmetastatic breast cancer cells. This suggests a possible scenario in which PKD1 silencing may lead to an increased level of SNAIL and a subsequent increase in the metastatic ability of cancer cells.

During cancer progression, the ubiquitylation and deubiquitylation system has been shown, in recent years, to play critical roles by aberrant signaling amplification (Zhang et al., 2012b), promoting survival (Lau et al., 2012; Zhao et al., 2008), and coping with DNA repair (Wu et al., 2012). Specifically, FBXO11 has also been identified to play multifaceted roles in cancer. In human B cell lymphoma, SCF-FBXO11 targets BCL6, a commonly overexpressed gene in aggressive diffuse large B cell lymphoma (DLBCL), for ubiquitylation and proteosomal degradation (Duan et al., 2012). Importantly, FBXO11 has been found to be deleted or mutated in multiple DLBCL cell lines, and inactivation of FBXO11 correlates with an increased level of BCL6. These observations suggest that FBXO11 may be an important tumor suppressor in DLBCL. More recently, SCF-FBXO11 has been shown to interact with CDT2, a DCAF protein that controls cell cycle progression, and to promote CDT2 proteosomal degradation. This regulatory mechanism also has important implications in cell cycle exit and cell migration (Abbas et al., 2013; Duan et al., 2012). Our study extended the multifaceted role FBXO11 in cancer from a tumor suppressor to a key metastasis inhibitor by suppressing SNAIL-mediated EMT, invasion, and metastasis.

EXPERIMENTAL PROCEDURES

Animal Studies

All procedures involving mice and experimental protocols were approved by Institutional Animal Care and Use Committee of Princeton University. For orthotopic primary tumor formation, female BALB/c mice or athymic nude mice 4-6 weeks of age were anesthetized, and a small incision was made to reveal the mammary gland. Tumor cells suspended in 10 μl PBS were injected directly into the mammary fat pad. The primary tumor growth was monitored weekly by measurement of tumor size. In a 4T1 FBXO11-KD lung metastasis assay, primary tumors were removed after 10 days. Lung metastasis nodes were examined after euthanizing the mice at the experimental endpoint.

Clinical Data Set Analysis

NKI295 gene expression data were downloaded from the Stanford Microarray Database. For E3 candidate survival analyses (*FBXO11*, *SPSB1*, and *SOCS3*), distant metastasis-free survivals, stratified by expression of the gene of interest, were presented as Kaplan-Meier plots and tested for significance using log rank tests in the NKI295 data set. The *TRIM5* gene was not included in the NKI295 data set, and, therefore, it was analyzed using the online KMplot database (http://www.KMplot.com) (Győrffy et al., 2010). A PKD1 survival analysis was also done in the KMplot database using relapse-free survival.

Human Breast Cancer Tissue Microarrays

Formalin-fixed, paraffin-embedded microarrays of breast cancer tissues were from US Biomax (BC081120) and from Sun Yat-Sen University Cancer Center. Both sample sets used deidentified tumor samples and were considered exempt by the institutional review boards of Princeton University and Sun Yat-Sen University Cancer Center.

Statistical Analysis

Results were reported as mean ± SD or mean ± SEM as indicated in the figure legends. Statistical comparisons were performed using unpaired two-sided Student's t test with unequal variance assumption. Statistical comparison for the 4T1 lung metastasis assay was performed using Mann-Whitney U test. Clinical correlation of SNAIL staining and lymph node invasion was performed using a χ^2 test. Clinical correlation between SNAIL and FBXO11 or between pY95-PKD1 and p-Ser-11 SNAIL was also performed using a χ^2 test. All experiments with representative images (including Western blot analysis and immunofluorescence) were repeated at least twice, and representative images are shown. The histology images in Figure 8 are representative of tumor specimens of the same category (SNAIL-high or SNAIL-low).

ACCESSION NUMBERS

The raw and normalized microarray data have been deposited in the Gene Expression Omnibus database under accession number GSE50889.

SUPPLEMENTAL INFORMATION

Supplemental Information includes Supplemental Experimental Procedures, seven figures, and two tables and can be found with this article online at http://dx.doi.org/10.1016/j.ccr.2014.07.022.

ACKNOWLEDGMENTS

We thank Dr. R.A. Weinberg for providing HMLEN cells and Dr. B.P. Zhou for providing the SNAIL-2SA, SNAIL-4SA, and SNAIL-6SA plasmids. We thank

Dr. M. Pagano for providing FLAG-tagged FBXO11, FBXO1, FBXO5, FBXO10, FBXO31, FBXW1, and FBXW9 and for helpful advice. We thank B. Ell, M.B. Esposito, B.I. Koh, L. Wan, R. Chakrabarti, and other laboratory members for helpful discussions; M. Yuan for technical assistance; and C. DeCoste for assistance with flow cytometry. We thank L. Cong at the Tissue Analytic Service Core of Cancer Institute of New Jersey for optimizing the conditions for IHC staining of clinical tumor samples. This research was supported by a CINJ Research Development Award; by the Brewster Foundation; and by grants from the U.S. Department of Defense (BC123187), the NIH (R01CA134519 and R01CA141062 to Y.K. and GM086435 and CA140182 to P.S.) and the National Science Foundation of China (to Y.K. and H-Y.W.),. H.Z. is a recipient of a Komen for the Cure postdoctoral fellowship (KG111164), and G. R. is a recipient of a DOD postdoctoral fellowship (BC123284). M.S. is supported by the 111 Project of China (B13026, Department of Education) and by an international exchange program of Zhejiang University.

Received: September 19, 2013
Revised: April 3, 2014
Accepted: July 24, 2014
Published: September 8, 2014

REFERENCES

Abbas, T., Mueller, A.C., Shibata, E., Keaton, M., Rossi, M., and Dutta, A. (2013). CRL1-FBXO11 promotes Cdt2 ubiquitylation and degradation and regulates Pr-Set7/Set8-mediated cellular migration. Mol. Cell. *49*, 1147–1158.

Bastea, L.I., Döppler, H., Balogun, B., and Storz, P. (2012). Protein kinase D1 maintains the epithelial phenotype by inducing a DNA-bound, inactive SNAI1 transcriptional repressor complex. PLoS ONE *7*, e30459.

Batlle, E., Sancho, E., Francí, C., Domínguez, D., Monfar, M., Baulida, J., and García De Herreros, A. (2000). The transcription factor snail is a repressor of E-cadherin gene expression in epithelial tumour cells. Nat. Cell Biol. *2*, 84–89.

Borges, S., Döppler, H., Perez, E.A., Andorfer, C.A., Sun, Z., Anastasiadis, P.Z., Thompson, E., Geiger, X.J., and Storz, P. (2013). Pharmacologic reversion of epigenetic silencing of the PRKD1 promoter blocks breast tumor cell invasion and metastasis. Breast Cancer Res. *15*, R66.

Brabletz, T. (2012). To differentiate or not—routes towards metastasis. Nat. Rev. Cancer *12*, 425–436.

Cano, A., Pérez-Moreno, M.A., Rodrigo, I., Locascio, A., Blanco, M.J., del Barrio, M.G., Portillo, F., and Nieto, M.A. (2000). The transcription factor snail controls epithelial-mesenchymal transitions by repressing E-cadherin expression. Nat. Cell Biol. *2*, 76–83.

Cardozo, T., and Pagano, M. (2004). The SCF ubiquitin ligase: insights into a molecular machine. Nat. Rev. Mol. Cell Biol. *5*, 739–751.

De Craene, B., and Berx, G. (2013). Regulatory networks defining EMT during cancer initiation and progression. Nat. Rev. Cancer *13*, 97–110.

Dong, C., Yuan, T., Wu, Y., Wang, Y., Fan, T.W., Miriyala, S., Lin, Y., Yao, J., Shi, J., Kang, T., et al. (2013). Loss of FBP1 by Snail-mediated repression provides metabolic advantages in basal-like breast cancer. Cancer Cell *23*, 316–331.

Du, C., Zhang, C., Hassan, S., Biswas, M.H., and Balaji, K.C. (2010). Protein kinase D1 suppresses epithelial-to-mesenchymal transition through phosphorylation of snail. Cancer Res. *70*, 7810–7819.

Duan, S., Cermak, L., Pagan, J.K., Rossi, M., Martinengo, C., di Celle, P.F., Chapuy, B., Shipp, M., Chiarle, R., and Pagano, M. (2012). FBXO11 targets BCL6 for degradation and is inactivated in diffuse large B-cell lymphomas. Nature *481*, 90–93.

Eiseler, T., Döppler, H., Yan, I.K., Kitatani, K., Mizuno, K., and Storz, P. (2009). Protein kinase D1 regulates cofilin-mediated F-actin reorganization and cell motility through slingshot. Nat. Cell Biol. *11*, 545–556.

Eiseler, T., Köhler, C., Nimmagadda, S.C., Jamali, A., Funk, N., Joodi, G., Storz, P., and Seufferlein, T. (2012). Protein kinase D1 mediates anchorage-dependent and -independent growth of tumor cells via the zinc finger transcription factor Snail1. J. Biol. Chem. *287*, 32367–32380.

Emanuele, M.J., Elia, A.E., Xu, Q., Thoma, C.R., Izhar, L., Leng, Y., Guo, A., Chen, Y.N., Rush, J., Hsu, P.W., et al. (2011). Global identification of modular cullin-RING ligase substrates. Cell *147*, 459–474.

Győrffy, B., Lanczky, A., Eklund, A.C., Denkert, C., Budczies, J., Li, Q., and Szallasi, Z. (2010). An online survival analysis tool to rapidly assess the effect of 22,277 genes on breast cancer prognosis using microarray data of 1,809 patients. Breast Cancer Res. Treat. *123*, 725–731.

Hennessy, B.T., Gonzalez-Angulo, A.M., Stemke-Hale, K., Gilcrease, M.Z., Krishnamurthy, S., Lee, J.S., Fridlyand, J., Sahin, A., Agarwal, R., Joy, C., et al. (2009). Characterization of a naturally occurring breast cancer subset enriched in epithelial-to-mesenchymal transition and stem cell characteristics. Cancer Res. *69*, 4116–4124.

Kudo-Saito, C., Shirako, H., Takeuchi, T., and Kawakami, Y. (2009). Cancer metastasis is accelerated through immunosuppression during Snail-induced EMT of cancer cells. Cancer Cell *15*, 195–206.

Lander, R., Nordin, K., and LaBonne, C. (2011). The F-box protein Ppa is a common regulator of core EMT factors Twist, Snail, Slug, and Sip1. J. Cell Biol. *194*, 17–25.

Lau, A.W., Fukushima, H., and Wei, W. (2012). The Fbw7 and betaTRCP E3 ubiquitin ligases and their roles in tumorigenesis. Front Biosci (Landmark Ed) *17*, 2197–2212.

Liu, N., Li, H., Li, S., Shen, M., Xiao, N., Chen, Y., Wang, Y., Wang, W., Wang, R., Wang, Q., et al. (2010). The Fbw7/human CDC4 tumor suppressor targets proproliferative factor KLF5 for ubiquitination and degradation through multiple phosphodegron motifs. J. Biol. Chem. *285*, 18858–18867.

Mani, S.A., Guo, W., Liao, M.J., Eaton, E.N., Ayyanan, A., Zhou, A.Y., Brooks, M., Reinhard, F., Zhang, C.C., Shipitsin, M., et al. (2008). The epithelial-mesenchymal transition generates cells with properties of stem cells. Cell *133*, 704–715.

Minn, A.J., Gupta, G.P., Siegel, P.M., Bos, P.D., Shu, W., Giri, D.D., Viale, A., Olshen, A.B., Gerald, W.L., and Massagué, J. (2005). Genes that mediate breast cancer metastasis to lung. Nature *436*, 518–524.

Momand, J., Zambetti, G.P., Olson, D.C., George, D., and Levine, A.J. (1992). The mdm-2 oncogene product forms a complex with the p53 protein and inhibits p53-mediated transactivation. Cell *69*, 1237–1245.

Moody, S.E., Perez, D., Pan, T.C., Sarkisian, C.J., Portocarrero, C.P., Sterner, C.J., Notorfrancesco, K.L., Cardiff, R.D., and Chodosh, L.A. (2005). The transcriptional repressor Snail promotes mammary tumor recurrence. Cancer Cell *8*, 197–209.

Muratani, M., and Tansey, W.P. (2003). How the ubiquitin-proteasome system controls transcription. Nat. Rev. Mol. Cell Biol. *4*, 192–201.

Nieto, M.A. (2011). The ins and outs of the epithelial to mesenchymal transition in health and disease. Annu. Rev. Cell Dev. Biol. *27*, 347–376.

Pon, Y.L., Zhou, H.Y., Cheung, A.N., Ngan, H.Y., and Wong, A.S. (2008). p70 S6 kinase promotes epithelial to mesenchymal transition through snail induction in ovarian cancer cells. Cancer Res. *68*, 6524–6532.

van de Vijver, M.J., He, Y.D., van't Veer, L.J., Dai, H., Hart, A.A., Voskuil, D.W., Schreiber, G.J., Peterse, J.L., Roberts, C., Marton, M.J., et al. (2002). A gene-expression signature as a predictor of survival in breast cancer. N. Engl. J. Med. *347*, 1999–2009.

Wan, L., Pantel, K., and Kang, Y. (2013). Tumor metastasis: moving new biological insights into the clinic. Nat. Med. *19*, 1450–1464.

Wu, J., Zhang, X., Zhang, L., Wu, C.Y., Rezaeian, A.H., Chan, C.H., Li, J.M., Wang, J., Gao, Y., Han, F., et al. (2012). Skp2 E3 ligase integrates ATM activation and homologous recombination repair by ubiquitinating NBS1. Mol. Cell *46*, 351–361.

Yang, Z., Rayala, S., Nguyen, D., Vadlamudi, R.K., Chen, S., and Kumar, R. (2005). Pak1 phosphorylation of snail, a master regulator of epithelial-to-mesenchyme transition, modulates snail's subcellular localization and functions. Cancer Res. *65*, 3179–3184.

Zhang, K., Rodriguez-Aznar, E., Yabuta, N., Owen, R.J., Mingot, J.M., Nojima, H., Nieto, M.A., and Longmore, G.D. (2012a). Lats2 kinase potentiates Snail1

activity by promoting nuclear retention upon phosphorylation. EMBO J. *31*, 29–43.

Zhang, L., Zhou, F., Drabsch, Y., Gao, R., Snaar-Jagalska, B.E., Mickanin, C., Huang, H., Sheppard, K.A., Porter, J.A., Lu, C.X., and ten Dijke, P. (2012b). USP4 is regulated by AKT phosphorylation and directly deubiquitylates TGF-β type I receptor. Nat. Cell Biol. *14*, 717–726.

Zhao, X., Heng, J.I., Guardavaccaro, D., Jiang, R., Pagano, M., Guillemot, F., Iavarone, A., and Lasorella, A. (2008). The HECT-domain ubiquitin ligase Huwe1 controls neural differentiation and proliferation by destabilizing the N-Myc oncoprotein. Nat. Cell Biol. *10*, 643–653.

Zhao, D., Zheng, H.Q., Zhou, Z., and Chen, C. (2010). The Fbw7 tumor suppressor targets KLF5 for ubiquitin-mediated degradation and suppresses breast cell proliferation. Cancer Res. *70*, 4728–4738.

Zhou, B.P., Deng, J., Xia, W., Xu, J., Li, Y.M., Gunduz, M., and Hung, M.C. (2004). Dual regulation of Snail by GSK-3beta-mediated phosphorylation in control of epithelial-mesenchymal transition. Nat. Cell Biol. *6*, 931–940.